

Convolution Effects in Superconductive Tunneling

J. Geerk¹ and H. v. Löhneysen^{1,2}

¹*Forschungszentrum Karlsruhe, Institut für Festkörperphysik, D-76021 Karlsruhe, Germany*

²*Physikalisches Institut, Universität Karlsruhe, D-76128 Karlsruhe, Germany*

(Received 12 July 2007; published 19 December 2007)

The quasiparticle density of states (DOS) of superconductors can be obtained from tunneling spectroscopy. When the normal-state differential conductance varies on the voltage scale comparable to that of strong-coupling effects, the standard normalization rule to extract the DOS is invalid, and the DOS is related to the measured data via an integral equation. These effects are exemplified by studying the geometry effect on the DOS for simple BCS superconductors. We apply these considerations to UPd₂Al₃ tunnel data where the apparent strong-coupling effects, previously deduced by use of the normalization rule, can be quantitatively attributed to convolution effects.

DOI: [10.1103/PhysRevLett.99.257005](https://doi.org/10.1103/PhysRevLett.99.257005)

PACS numbers: 74.50.+r, 74.25.Kc, 74.70.Ad

Electron tunneling provides a detailed picture of the superconducting state as first demonstrated by McMillan and Rowell [1] for the strong-coupling superconductor Pb. The differential conductance dI/dV as a function of applied voltage V yields the quasiparticle density of states (DOS) in the superconducting state as modified by strong-coupling effects. Hence, the tunneling experiment can address the mechanism of Cooper-pair coupling, which so far in most cases resulted in phonons as the mediating boson. The discovery of superconductivity in heavy-fermion (HF) systems, high-temperature superconducting cuprates (HTSC), and ruthenates prompted alternative pairing scenarios and numerous tunneling investigations. As an important example, Jourdan *et al.* [2] presented tunnel data on thin films of the HF superconductor UPd₂Al₃ and concluded that the coupling is mediated by antiferromagnetic spin fluctuations. On the basis of these and additional inelastic neutron-scattering (INS) data, a magnetic exciton of an energy near 1 meV was suggested as coupling boson [3,4]. In view of the strong impact of this work on the issue of unconventional superconductivity in general, we felt motivated to investigate in detail the conditions for a reliable extraction of the superconductive DOS from tunnel data.

Compared to the large number of experiment data, the evaluation procedures and the effect of the geometry on the tunnel data have found marginal attention. Detailed theoretical analyses of tunneling data of unconventional superconductors have only appeared recently [5,6]. We present in this Letter a thorough account of how to extract superconductive properties. In particular, care has to be taken when employing as counterelectrode a conventional superconductor that is driven normal by a suitable magnetic field. Studying conventional s -wave superconductors, we find a strong dependence of the conductance on the geometry of the tunnel junctions employed, which arises from penetration-depth effects and can be analyzed by proper deconvolution of the tunneling data.

Usually, a tunnel junction is composed of two electrodes separated by the tunnel barrier, with electrode 1 made of the material of interest, often in the form of a thin film, and a suitable counterelectrode 2. For the latter, mostly s - p metals that can be easily evaporated are used, such as Pb and In. When in the superconducting state, they allow a detailed analysis of the junction quality including leakage currents, foreign phase contents, and Josephson effects. In order to determine the superconductive DOS, $N_T(V)$, of the material of interest, the superconductivity of the counterelectrode is suppressed by applying a small magnetic field. The quantities to be determined are the differential conductances of the junction in the superconducting and normal state of the material of interest, $g_s(V)$ and $g_n(V)$, respectively. A straightforward procedure yields $N_T(V)$ in the form of a simple normalization formula [1]

$$N_T(V) = g_s(V)/g_n(V). \quad (1)$$

To outline the limitations of Eq. (1), we employ the general expression for the tunnel current [7] of a junction at sufficiently low temperature with electrode 1 in the superconducting state

$$I_s(V) = \int_0^V A(E, V) N_T(E) dE. \quad (2)$$

Here, $A(E, V)$ contains all possible energy (or voltage) dependencies other than $N_T(E)$, like that of the tunnel matrix element, DOS effects of the barrier and the counterelectrode, and inelastic tunneling. For the quantities $g_s(V)$ and $g_n(V)$, it follows (Leibniz rule),

$$g_s(V) = A(V, V) N_T(V) + \int_0^V N_T(E) \frac{\partial A(E, V)}{\partial V} dE, \quad (3)$$

$$g_n(V) = A(V, V) + \int_0^V \frac{\partial A(E, V)}{\partial V} dE. \quad (4)$$

Hence, $N_T(V)$ is, in fact, connected to g_s and g_n via a complicated implicit equation. Obviously, the normaliza-

tion rule Eq. (1) is valid only if $A(E, V)$ and hence $g_n(V)$ vary slowly enough that the integrals in Eqs. (3) and (4) can be neglected. The error introduced by applying Eq. (1) scales with the difference of the integrals which is determined mainly by the properties of $N_T(E)$ in the energy gap region.

For a solution of Eqs. (3) and (4), we have to proceed with reasonable assumptions for the functional form of $A(E, V)$. The tunneling matrix element varies usually slowly in the spectroscopic voltage range [7], and we neglect its effect in the following considerations. Among the effects that generate fine structure in $g_n(V)$, comparable to possible strong-coupling effects in $N_T(V)$, are DOS effects of both electrodes and inelastic tunneling.

These effects can be expressed in two special forms of $A(E, V)$. For the first case, $A(E, V) = A(E)$, the normalization rule is trivially valid as we constructed $A(E, V)$ to depend on the voltage scale of electrode 1 only and to be independent of the superconducting state of electrode 1. Possible examples are bandstructure effects as observed in semimetals or degenerate semiconductors, or many-particle effects like a Coulomb gap [8,9].

The second case, $A(E, V) = A(E - V)$, describes, e.g., DOS effects connected to the voltage scale of the counterelectrode 2. These are directly displayed in $g_n(V)$, while inelastic tunneling is reflected in $g_n(V)$ via an integral function of the effective barrier spectrum. Equation (2), a Volterra equation of the first kind, reduces to the Laplacian convolution, yielding

$$g_s(V) = A(0)N_T(V) - \int_0^V N_T(E) \frac{\partial A(E - V)}{\partial E} dE, \quad (5)$$

$$g_n(V) = A(-V). \quad (6)$$

Obviously, for a given $g_s(V)$ and $g_n(V)$, the $N_T(V)$ data obtained for case 1 or case 2 can differ strongly while at the same time the different physical situations underlying the two cases may be difficult to identify. Inelastic effects implying case 2 can be identified by their strong temperature broadening [10]. Brinkman and Tsui [11] used Eqs. (5) and (6) to analyze Pb/I/Si tunnel junctions accounting for bandstructure effects of the Si counterelectrode.

A simplified correction procedure can be used for junctions of case 2 if the relative variation of $g_n(V)$ is small within the voltage range of interest. As discussed above, the convolution integral is mainly determined by $N_T(V)$ in the gap region and, for s -wave superconductors, can be well approximated by the BCS form $N_T^{\text{BCS}}(V)$. Thus, we obtain from Eqs. (5) and (6)

$$N_T(V) = g_s(V)/g_n^{\text{corr}}(V) \quad (7)$$

with

$$g_n^{\text{corr}}(V) = g_n(0) + \int_0^V N_T^{\text{BCS}}(V) \frac{\partial g_n(V - E)}{\partial E} dE. \quad (8)$$

$g_n^{\text{corr}}(V)$ is a normal-state background that has a point-by-

point relation to $g_s(V)$ and hence obeys the normalization rule for $N_T(V)$. This procedure was used by Rowell [12] for the correction of $g_n(V)$ data with respect to inelastic effects, which is indispensable for the evaluation of tunnel data involving optical phonons [13–15].

For $g_n(V)$ data with a fine structure of unknown origin, a test calculation facilitates the discrimination between the two cases: Inserting $N_T^{\text{BCS}}(V)$ on the right-hand side of Eq. (5) yields $g_s^{\text{calc}}(V)$ to be compared to the measured $g_s(V)$. A similarity with the Laplacian convolution [Eq. (5)] would imply that the junction follows case 2.

In the following, we will present tunneling experiments that illustrate the convolution effects, by studying the field dependence of a rather simple $S/I/S'$ structure where both S and S' are conventional superconductors, albeit with strongly differing (bulk) critical fields. Here, structure in $g_n(V)$ arises from geometry effects, i.e., the thickness dependence of the (upper) critical field B_c in the nominally low- B_c superconductor S' . For films thinner than the London penetration depth λ_L , very high fields are necessary to fully suppress superconductivity [16]. For instance, Al/Al₂O₃/Pb tunnel junctions with a Pb film thickness of $14 \text{ nm} < \lambda_L^{\text{Pb}} = 50 \text{ nm}$, still show the full energy gap of Pb at a field of 1.5 T [17].

We prepared tunnel junctions on Ta films alloyed with 1.5 at% of Mo. Compared to pure Ta ($T_c = 4.4 \text{ K}$, $B_c = 0.083 \text{ T}$), the Mo alloying reduces T_c to 3.7 K, but strongly enhances the critical field with first signs of a degradation of the tunneling gap appearing around 0.3 T. Hence, this film is fully superconducting in fields up to 0.2 T which were applied to suppress superconductivity in the Pb counterelectrode. After oxidation in air of the Ta-Mo film, the Pb film was evaporated using three different geometries, but keeping always the size of roughly $0.5 \times 0.5 \text{ mm}^2$ for the junction area: (A) the junction area was defined by a varnish mask on the oxidized Ta-Mo film leaving a window of $0.5 \times 0.5 \text{ mm}^2$. For B and C, junctions in cross-strip geometry were fabricated [18]. (B) the Pb film strip (width 0.5 mm) was evaporated through a mask with the long axis perpendicular to that of the underlying Ta-Mo film and in close contact ($\leq 0.05 \text{ mm}$) the latter. (C) same as B with the mask positioned 1 mm away from the Ta-Mo film.

Data for geometry A are shown in Fig. 1. The Pb film of about 300 nm thickness covers the window completely so that no film fringes are in contact with the junction area. We observe already for $B = 0.089 \text{ T}$ extensive suppression of superconductivity of the Pb film, which is complete for 0.2 T where the conductance data are identical to those from a junction with an In counterelectrode that is fully in the normal state at 0.2 T.

The data for the junctions with cross-strip geometries B and C are shown in Fig. 2. We first discuss C where, due to the large distance between the mask and the Ta-Mo surface, the resulting Pb film shows a thickness variation $d(x)$ extending over the whole width of the film with $d < \lambda_L^{\text{Pb}}$ for a large part. In comparison with the 0.2 T data of Fig. 1, the

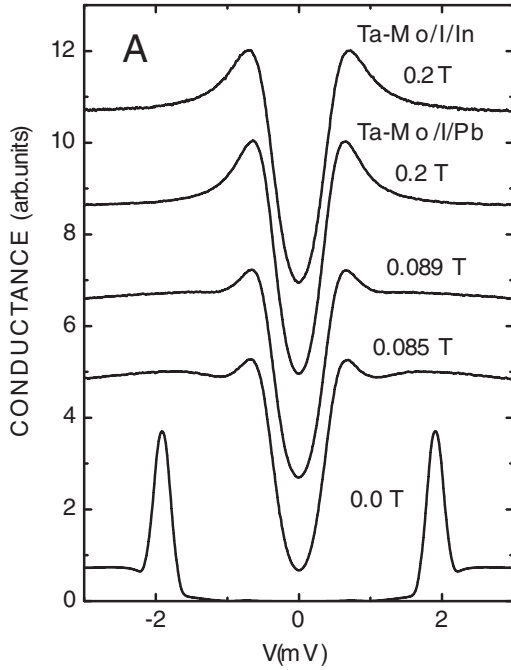


FIG. 1. Conductance data taken at 1.2 K at different magnetic fields of a Ta-Mo/I/Pb tunnel junction prepared using a window technique (geometry A, see text) for different magnetic fields applied parallel to the junction surface. Traces were shifted for clarity; the upper one is obtained from a junction with In counterelectrode.

maximum in $g_s(V)$ appears at much higher voltage which is characteristic of a $S/I/S'$ type junction. We determined an effective DOS of the Pb film by calculating $g_n(V)$ from Eqs. (5) and (6) (using for $N_T(V)$ the 0.2 T data from the junction with geometry A). This $g_n(V)$ trace reveals that indeed at 0.2 T, the major part of the Pb film remains in the superconducting state. In the upper part of Fig. 2, we show data of a junction with geometry B, resembling the geometry described by Jourdan *et al.* [2]. Here the film edges make up only a small part of the Pb film. The data are similar to the 0.2 T data of Fig. 1 but with additional features roughly 1.1 mV above the gap edge of the Ta-Mo film. Obviously, these features can be misinterpreted as strong-coupling effects in the DOS of the Ta-Mo film. The effective DOS of this Pb film shows a normal (gapless) state for about 95% of the film, corresponding to the part with nominal thickness. This tunnel current superimposes with that through the film edges remaining in the superconducting state to form the valleylike shape that is similar to the normal-state data determined at 0.3 K on the UPd₂Al₃/I/Pb junctions [19].

For the test calculation—as outlined above—for the data of Jourdan *et al.* [2], $g_n(V)$ data are in fact available [19]. A weak-coupling BCS DOS with a gap of 0.23 meV, broadened as described by Jourdan *et al.* [2], was convoluted with the valleylike $g_n(V)$, given in Ref. [19]. The resulting curve $g_s^{\text{calc}}(V)$ (solid line in Fig. 3) shows an oscillation near 1.2 mV in close agreement with the mea-

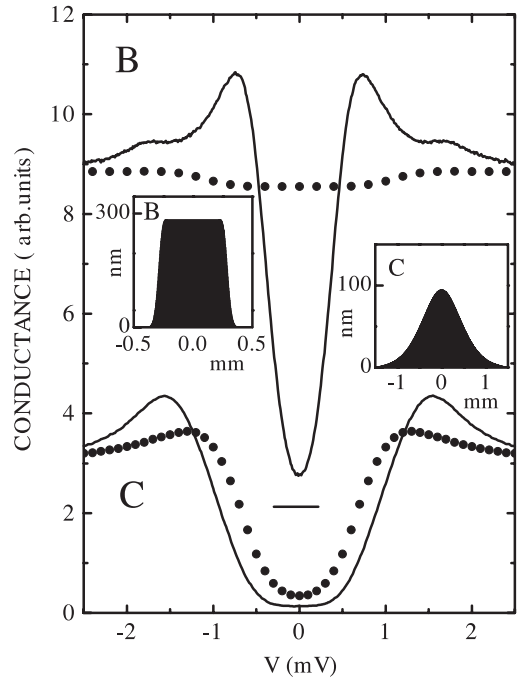


FIG. 2. Conductance data (solid lines) taken at 1.2 K and 0.2 T for Ta-Mo/I/Pb junctions prepared in cross-strip geometry along the long axis of the underlying Ta-Mo film. Mask position B (upper set of data) and C (lower set of data). Insets sketch the resulting Pb thickness profiles. Dots show the effective DOS $g_n(V)$ of the Pb films (see text for details).

sured data [2] (open squares in Fig. 3). A similar feature of a HTSC superconductive DOS convoluted with steplike g_n data caused by inelastic tunneling was discussed recently [5]. Furthermore, we use $g_s^{\text{calc}}(V)$, normalize it by the 1.7-K normal-state data, and compare the result with the BCS DOS in the inset of Fig. 3. It agrees strikingly well with the analogous data shown in the inset of Fig. 3 in Ref. [2], underscoring that indeed case 2 discussed above is appropriate for the UPd₂Al₃ data, allowing to extract $g_n^{\text{corr}}(V)$ from measured data according to Eq. (8) (cf open circles in Fig. 3). We observe that the maximum at 1.3 mV appearing in the $g_s(V)$ data also shows up in the g_n^{corr} data. It is generated by the Laplacian convolution in Eq. (8), its shape reflecting the peak at the gap edge of $N_T^{\text{BCS}}(V)$ scaled down by the relative strength of the valleylike anomaly of $g_n(V)$. In accordance with the findings presented above, $N_T(V)$ resulting from the $g_s(V)$ and $g_n^{\text{corr}}(V)$ data very closely resembles to weak-coupling BCS behavior.

As a final point, we briefly discuss the implications of our work for the superconducting properties of UPd₂Al₃. A consistent picture of the tunneling data with a magnetically mediated Cooper-pair coupling must take the relevant energy scales into account. The magnetic exciton picture of Sato *et al.* [3] suggests the broad dispersive feature observed in INS at an energy of 1.4 meV as the coupling boson. In the frame of Eliashberg theory, this coupling should lead to a positive deviation of $g_s(V)$ from the

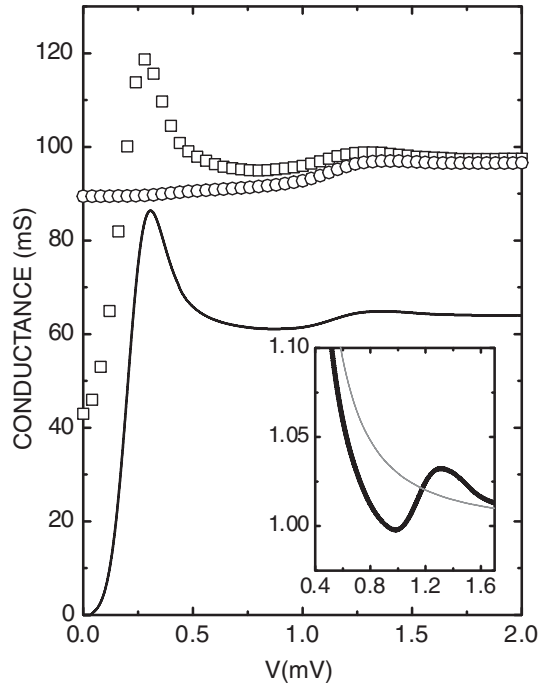


FIG. 3. Conductance $g_s^{\text{calc}}(V)$ resulting from a convolution of an assumed weak-coupling BCS DOS for UPd_2Al_3 with the valleylike normal state from Ref. [19] (solid line). For comparison, the measured superconductive $g_s(V)$ [2,19] is also shown (open squares). The normal-state background corrected for convolution effects $g_n^{\text{corr}}(V)$ (open circles). Inset shows $g_s^{\text{calc}}(V)$ normalized to the 1.7-K normal-state data (thick line) compared to the BCS DOS, analogous to Fig. 3 of Ref. [2].

BCS DOS followed by a downward step at 1.4 meV—the energy of the coupling boson—above Δ_0 . A positive “overswing” occurs at an energy about 3 times higher (4 to 5 meV). This has been observed in numerous analogous examples of strong electron-phonon coupling, e.g., for lead [1], and in fact also calculated by Sato *et al.* [3]. However, the tunneling data of Jourdan *et al.* [2] exhibit the “overswing” at much lower voltage, i.e., at 1 meV above Δ_0 , while the downward step with increasing V is not seen at all. It may, however, be masked by the rapidly decreasing BCS DOS. Hence, even if the features observed by Jourdan *et al.* [2] are to be attributed to a coupling boson, its energy would have to be much smaller than the broad feature seen in INS. We further note that this model assumes a two-component $5f$ electron picture, with two $5f$ electrons per U^{4+} site localized, carrying a local magnetic moment, and one electron being delocalized. While this picture receives a basis from a number of different experiments, a recent high-resolution neutron spin-echo study [20] suggests that a Fermi surface with all-itinerant $5f$ electrons is consistent with the observed inelastic neutron scattering. Clearly, more work is necessary to unravel the Cooper pairing in UPd_2Al_3 completely.

In conclusion, we have deduced the normalization rule of tunneling spectroscopy from the general expression of

the tunnel current and outlined the criterion of validity of this simple evaluation procedure. In case of an energy-dependent (normal-state) DOS and/or inelastic tunneling, the relation between the measured data and the superconductive DOS is described by an integral equation. The procedure is exemplified by an experimental study on simple superconductors. A critical analysis of tunnel data of the heavy-fermion UPd_2Al_3 superconductor [2] provides compelling evidence against an unequivocal assignment of strong-coupling features. We suggest that tunneling data on novel superconductors be analyzed according to the procedures outlined above in order to obtain reliable information on Cooper pairing and coupling strength.

-
- [1] W.L. McMillan and J.M. Rowell, in *Superconductivity*, edited by R.D. Parks (Decker, New York, 1969), p. 561.
 - [2] M. Jourdan, M. Huth, and H. Adrian, *Nature (London)* **398**, 47 (1999).
 - [3] N.K. Sato, N. Aso, K. Miyake, R. Shiina, P. Thalmeier, G. Varelogiannis, C. Geibel, F. Steglich, P. Fulde, and T. Komatsubara, *Nature (London)* **410**, 340 (2001).
 - [4] P. McHale, P. Fulde, and P. Thalmeier, *Phys. Rev. B* **70**, 014513 (2004).
 - [5] S. Pilgram, T.M. Rice, and M. Sigrist, *Phys. Rev. Lett.* **97**, 117003 (2006).
 - [6] D. Parker and P. Thalmeier, *Phys. Rev. B* **75**, 184502 (2007).
 - [7] W.F. Brinkman, R.C. Dynes, and J.M. Rowell, *J. Appl. Phys.* **41**, 1915 (1970).
 - [8] J.J. Hauser and L.R. Testardi, *Phys. Rev. Lett.* **20**, 12 (1968).
 - [9] M. Lee, J.G. Massey, V.L. Nguyen, and B.I. Shklovskii, *Phys. Rev. B* **60**, 1582 (1999).
 - [10] J. Lambe and R.C. Jaklevic, *Phys. Rev.* **165**, 821 (1968).
 - [11] W.F. Brinkman and D.C. Tsui, *Phys. Rev. B* **6**, 1063 (1972).
 - [12] J.M. Rowell, in *Tunneling Phenomena in Solids*, edited by E. Burstein and S. Lundqvist (Plenum, New York, 1969), Chap. 2.
 - [13] J. Geerk, U. Schneider, W. Bangert, H. Rietschel, F. Gompf, M. Gurvitch, J. Remeika, and J.M. Rowell, *Physica B+C (Amsterdam)* **135B**, 187 (1985).
 - [14] J. Geerk, G. Linker, and R. Smithey, *Phys. Rev. Lett.* **57**, 3284 (1986).
 - [15] J. Geerk, R. Schneider, G. Linker, A.G. Zaitsev, R. Heid, K.-P. Bohnen, and H. v. Löhneysen, *Phys. Rev. Lett.* **94**, 227005 (2005).
 - [16] P. Fulde, *Adv. Phys.* **22**, 667 (1973).
 - [17] R. Meservey and P.M. Tedrow, *Phys. Rev. B* **11**, 4224 (1975).
 - [18] P.M. Tedrow and R. Meservey, *Phys. Rev. B* **25**, 171 (1982).
 - [19] M. Huth, M. Jourdan, and H. Adrian, *Physica (Amsterdam)* **281 & 282B**, 882 (2000).
 - [20] E. Blackburn, A. Hiess, N. Bernhoeft, M.C. Rheinstädter, W. Häußler, and G.H. Lander, *Phys. Rev. Lett.* **97**, 057002 (2006).